Characterization and role of Helix contactin-related proteins in cultured Helix pomatia neurons

Characterization and role of *Helix* contactin-related proteins in cultured *Helix pomatia* neurons

C. Milanese[1]*, C. Giachello[1], F. Fiumara[1], A. Bizzoca[2], G. Gennarini[2], P.G. Montarolo[1,3], M. Ghirardi[1,3]

[1]Department of Neuroscience, University of Torino, Torino, Italy
[2]Department of Pharmacology and Human Physiology, University of Bari, Bari, Italy
[3]Istituto Nazionale di Neuroscienze, Torino, Italy

*Correspondence to: Dr. Chiara Milanese, Department of Neuroscience, University of Torino, Corso Raffaello 30, 10125 Torino, Italy. E-mail: chiara.milanese@unito.it

Abstract

We report on the structural and functional properties of the *Helix* contactin-related proteins (HCRPs), a family of closely related glycoproteins previously identified in the nervous system of the land snail *Helix pomatia* through antibodies against the mouse F3/contactin glycoprotein. We focus on HCRP1 and HCRP2, soluble FNIII domains-containing proteins of 90 and 45 kD bearing consensus motifs for both N- and O-glycosylation. Using the anti-HCRPs serum, we find secreted HCRPs in *Helix* nervous tissue isotonic extracts and in culture medium conditioned by *Helix* ganglia. In addition, we demonstrate expression of HCRPs on neuronal soma and on neurite extensions. Functionally, in *Helix* neurons, the antisense HCRP2 mRNA counteracts neurite elongation, and the recombinant HCRP2 protein exerts a strong positive effect on neurite growth when used as substrate. These data point to HCRPs as novel neurite growth-promoting molecules expressed in invertebrate nervous tissue.

Key words: neuronal growth factor; neurite elongation; F3/contactin

The neuronal surface expresses a large set of glycoproteins mediating the control of distinct aspects of neuronal physiology, including cell contact formation, neurite growth, fasciculation, pathfinding (Maness and Schachner,2007; Mann and Rougon,2007; Shapiro et al.,2007), synaptogenesis and synaptic function (Gerrow and El-Husseini,2006; Latefi and Colman,2006; Lardi-Studler and Fritschy,2007; Yamada et al.,2007). In spite of a large body of structural and functional studies, a full understanding of the role of these molecules is still largely incomplete, mostly because of the absence of useful biological models.

Several reports indicate that invertebrate nervous tissue represents an adequate tool with which to address these topics (Schacher et al.,2000; Wang et al.,2005; Kristiansen et al.,2005; Colon-Ramos et al.,2007; Funada et al.,2007; Li et al.,2007). In particular, in *Aplysia californica* and *Helix pomatia* nervous tissues, specific hints about the function of several adhesive glycoproteins have been obtained, including the *Aplysia* hortologue of the neural cell adhesion molecule (ApCAM; Mayford

et al.,1992; Schacher et al.,2000; Ghirardi et al.,2001) and a family of F3/contactin-related glycoproteins called "*Helix* contactin-related proteins" (HCRPs; Milanese et al.,2008).

In vertebrate neural development, F3/contactin is involved in axonal growth (Gennarini et al.,1991; Durbec et al.,1992; Bizzoca et al.,2003), fasciculation, and pathfinding (Berglund et al.,1999). In addition, this molecule undergoes complex interactions at the nodal/paranodal regions (Dupree et al.,1999, Boyle et al.,2001; Gollan et al.,2003), which correlates with a role in myelination. Together, these data account for a F3/contactin involvement in complex neural functions, as demonstrated in the cerebellum by in vivo approaches aimed at silencing the underlying gene (Berglund et al.,1999) or at modifying its expression profile (Bizzoca et al.,2003; Coluccia et al.,2004).

In a previous study, mouse F3/contactin antibody-inhibition approaches revealed that HCRPs share part of these functions, including the control of neuronal adhesion to the substrate and of axonal growth; in addition, these molecules play a role in neurotransmitter release (Milanese et al., 2008). In the same study, HCRPs were found to include different glycosylated peptides, ranging in size from 90 to 240 kD. Although differences in sugar content may contribute to this heterogeneity, the complex HCRPs profile could also reflect the existence of protein isoforms generated from translation of different mRNAs. In the present work, we explore this subject through the isolation and characterization of the HCRPs full-length cDNAs. In addition, we further investigate the significance of HCRPs expression in neuronal functions such as cell substrate adhesion and neurite elongation.

MATERIALS AND METHODS

Cell Culture

The technique for culturing *Helix* neurons has been previously described by Ghirardi et al. (1996). C1/C3, and B2 neurons from the cerebral and buccal ganglia, respectively, of juvenile animals were individually dissociated using a thin glass micropipette and plated in plastic dishes previously coated with different substrates. Cells were cultured at 18°C in L15 Leibovitz (Sigma Aldrich, St. Louis, MO) medium with appropriate salt concentrations (Ghirardi et al., 1996). Soma-to-soma paired neurons in culture were obtained as previously described (Fiumara et al., 2005) in L15 medium.

Substrate Preparation

Where not otherwise indicated, plastic dishes (Becton Dickinson, San Jose, CA) were coated with poly-L-lysine (0.1 mg/ml in sterile H2O; Sigma) and incubated in *Aplysia hemolymph* for 24 hr. For neurite growth assays, 10–20 μl of purified HCRP2 (0.2 μg/μl) or, alternatively, poly-L-lysine (0.1 mg/ml) was distributed over the plastic culture area, and then, after a 2-hr incubation at room temperature (RT), the dishes were washed several times with sterile H2O before use.

Preparation of *Helix pomatia* Conditioned Medium

Ganglia-conditioned medium (CM) was obtained from *Helix pomatia* nervous ganglia incubated in defined L15 medium (five or six ganglionic rings/ml for 72 hr) prepared according to Fiumara et al. (2005).

One to two milliliters of CM was concentrated (50×) with 3K Nanosep Centrifugal devices (Pall Corporation, East Hills, NY), following the manufacturer's protocol. Concentrated CM was then analyzed by Western blotting on 10% polyacrylamide gels as described by Milanese et al. (2008).

PF3 primary antiserum or preimmune serum (both 1:1,000 dilution in saturation buffer) was used, followed by HRP-labelled goat anti-rabbit IgG and the chemiluminescent ECL system (GE Healthcare, Piscataway, NJ).

Antiserum

The PF3 rabbit antiserum was generated against a 15-amino acid HCRP1 sequence (residues 111–125) coupled to keyhole limpet hemocyanin (Inalco, Milan, Italy), and the anti-HCRP2 rabbit antiserum was obtained against the 316–330-amino acid residues of HCRP2 (Inalco).

Immunocytochemistry

Cells were fixed with 4% paraformaldehyde in PBS for 40 min at RT and, after bleaching with 0.6% H2O2 in ethanol, incubated in blocking buffer (5% BSA in PBS 0.01 M). Then, the PF3 antiserum or the corresponding preimmune serum (both 1:100 dilution in blocking buffer) was added and incubated 1 hr at RT or overnight (ON) at 4°C. TRITC-conjugated goat anti-rabbit secondary antibodies (Jackson Laboratories; Bar Harbor, ME) were then applied (1:100 dilution in blocking buffer, 1 hr at RT). To evaluate its specificity, the PF3 serum was preabsorbed with the immunogenic peptide ON at 4°C (120 μg peptide in 500 μl of a 1:100 antiserum dilution in PBS) before the immunostaining procedures.

In the antisense microinjection experiments, after fixation and saturation as described above, cells were incubated ON at 4°C with the anti-HCRP2 serum or preimmune serum (1:500 dilution in blocking buffer), and the TRITC-conjugated goat secondary antibody was applied at a 1:400 dilution in blocking buffer for 1 hr at RT. Labelled cells were then observed with fluorescence optics and the images digitally analyzed in Image ProPlus software (Media Cybernetics, Bethesda, MD).

Immunohistochemistry

Immunohistochemical staining was performed as described by Milanese et al. (2008). PF3 antibody and the secondary biotinylated goat anti-rabbit serum (Vector Laboratories, Burlingame, CA) were used at 1:1,000 and 2 μg/ml dilutions, respectively.

Biochemical Procedures

Isotonic fractions were obtained by homogenizing whole Helix ganglia with 20 mM Tris/HCl, pH 8, containing 1% NP40 and protease inhibitors mix (Complete Mini; Roche, Indianapolis, IN). The soluble fraction was separated by centrifugation, and the membranes arising were suspended in RIPA buffer (50 mM Tris/HCl, pH 7.4, containing 1% NP40 and protease inhibitors). After a 10-min incubation on ice, the homogenate was centrifuged at 4°C, and the supernatant was boiled for 2 min in an equal volume of 2× Laemmli electrophoresis sample buffer.

Both fractions were then analyzed by Western blots. Samples containing 30 μg protein were separated on a 7% or 10% polyacrylamide gel and transferred to nylon membranes before being probed with the primary antiserum (PF3; 1:1,000 dilution in saturation buffer) or a rabbit preimmune serum (same dilution).

Rapid Amplification of cDNA Ends (RACE)

Full-length cDNA encoding the HCRP1 sequence was obtained by 3′- and 5′RACE, using the Generacer Kit (Invitrogen, Carlsbad, CA). Four micrograms of total RNA from *H. pomatia* ganglia were reverse transcribed using the Superscript II RT (Invitrogen) with the oligo-dT or GSP 5′REV

(5′-ccagaactgtgtctggactcaccggaat-3′) primers. The 3′RACE was performed through the 9.1 FW CTR (5′-ggacagagcgcaaaacggcgccaaa-3′) and NEST FOR 3′ (5′-gagctattccggtgagtccagacacagtt-3′) sense primers, both deduced from the sequence of clone 9.1 (Milanese et al.,2008) and the GeneRacer 3′ provided by the kit. For the 5′RACE, GSP 5′REV and NEST 5′REV: 5′-tgcctgatcgatctgtatggcatcggtaa-3′ reverse primers were used in combination with the GeneRacer 5′ primer. In all the amplification reactions, Platinum Taq DNA Polymerase High Fidelity (Invitrogen) was used. The PCR products were purified by gel electrophoresis and cloned in the pGEM-T vector (Promega, Madison, WI).

Isolation of HCRP2-cDNA From a Lambda Expression Library

A custom cDNA λTriplEx2 expression library, generated from *Helix* ganglia mRNA by oligo(dT) priming (Clontech, Mountain View, CA), was screened with a [a32P]dCTP (GE Healthcare)-labeled 980-bp probe from clone 9.1 (Milanese et al.,2008). Isolated phages were converted in pTriplEx2 plasmids by cre-LoxP recombination mediated at LoxP sites of λTriplEx2 and sequenced. (AGOWA, Berlin, Germany).

Sequence Analysis

Sequences were analyzed through the protein database search program BLAST (http://ncbi.nlm.nih.gov/BLAST) and the local alignment program LALIGN (http://workbench.sdsc.edu/). Multiple alignments were done with the CLUSTALW program (http://workbench.sdsc.edu/). Open reading frames were deduced with the ORF finder (http://www.ncbi.nlm.nih.gov/gorf.html), and protein structure was analyzed at the SMART (http://smart.embl-heidelberg.de/) sites. Potential N-glycosylation and O-glycosylation consensus sites were identified with the NetNGlyc and NetOGlyc programs, respectively, of the ExPASy proteomic tool (http://cbs.dtu.dk/services/NetNGlyc; http://cbs.dtu.dk/services/NetOGlyc).

Glutatione S-Transferase (GST)-HCRP2 Fusion Protein Production

GST-HCRPs fusion proteins were produced according to Frangioni et al. (1993). Full-length cDNA encoding HCRP2 (fragment EcoRI/XhoI, 910 bp) was cloned into the pGEX-6p-3 vector downstream the GST sequence (GE Healthcare). GST fusion protein expression was induced in the BL21 *Escherichia coli* cell line with 0.2 mM IPTG. Recombinant protein was then purified from bacterial lysate with a GSH-sepharose column (GE Healthcare), and GST tags were removed with the Prescission Protease enzyme (GE Healthcare) according to the manufacturer's protocol.

Transfection Procedures

The bicistronic vector pIRES-EGFP (Clontech) was used for generating CMV promoter-HCRPs cDNA expression vectors that included an enhanced green fluorescent protein (EGFP) reporter downstream of internal ribosomal entry sequence (IRES). Transient transfection was performed in LR73 CHO cells (Pollard and Stanners,1979) using DOTAP-liposomal transfection reagent (Roche), according to the manufacturer's protocol. Forty-eight hours after transfection, cells were fixed in 4% paraformaldehyde (40 min at RT) and saturated with 3% BSA in PBS for 45 min before incubation with the PF3 serum (1:200 dilution in blocking solution). A Cy3-conjugated goat anti-rabbit secondary antibody (Jackson Laboratories, 1:300 dilution) was then added. pIRES-EGFP vector alone was used as a positive control for the transfection reaction and sterile water as the negative control. Labelled cells were observed with fluorescence optics, and images were acquired with an intensified CCD camera.

In Vitro Transcription and Intracellular Injection of mRNA

To produce template DNAs for in vitro transcription, the HCRP2 cDNA was cloned into the PCS2+ vector (Promega), and antisense mRNA was generated from the SP6 promoter by the RiboMAX Large Scale RNA Production System (Promega). For intracellular antisense mRNA injection, cultured C1 and C3 neurons, collected from the *H. pomatia* cerebral ganglia, were plated on poly-L-lysine-treated substrates and allowed to grow for 6–12 hr before being injected. Microelectrode tips were filled with 0.5 μl of 0.4 M KCl containing HCRP2 antisense mRNA (0.5 μg/μl). After impalement, the neurons were loaded with short pressure pulses (10–20 pulses of 0.3–0.5 sec at 2–20 psi) delivered through a pneumatic picopump (PV820; WPI, Sarasota, FL) connected to the electrode holder. The injection procedure was monitored under visual and electrophysiological control.

Single-Cell RT-PCR

To verify the inhibitory effect exerted by the HCRP2 antisense on neurite growth, control and antisense-treated neurons were individually collected immediately after the injection and at the following 24 and 48 hr time points in 0.5 μl RNasin (40 U/μl; Promega) and immediately stored at –80°C. Total RNA from each single cell was subjected to cDNA synthesis (Im-Prom II reverse transcriptase; Promega) with oligo-dT as a primer. Five microliters of the resulting cDNA was used as template for HCRP2 (forward primer, 5′-ctgttggtggtgatttggtgg-3′; reverse primer, 5′-gcgcagtttgtccactttgtc-3′; 35 cycles) and for the *Helix* synapsin (forward primer, 5′-cggtgtacccagcatcaact-3′; reverse primer, 5′-cgatgaacggttctgtcgta-3′; 35 cycles), used as a control of the amplification reaction performed with the AccuPrime Taq DNA polymerase (Invitrogen). PCR products were run on a 2% agarose gel stained with ethidium bromide (Bio-Rad, Hercules, CA) in the presence of the DNA Molecular Weight Marker VIII (Roche).

Electrophysiological Recordings

Conventional electrophysiological techniques were used for intracellular recording of the synaptic activity of B2–B2 synapses, as previously reported (Fiumara et al.,2005). The synapses were electrophysiologically recorded 24 hr after cell–cell pairing on HCRP2 or poly-L-lysine substrate and analyzed accordingly to Fiumara et al. (2007).

Measurements of Neurite Length

For neurite length measurements, phase-contrast images of the cultures were acquired in Image Pro Plus with a Sony camera. Measurement of neurite length was made on extensions originating from the axonal stumps. For this purpose, a circumferential line, centered at the tip of the stump and interconnecting the tips of the three longest neurites, was drawn in a semiautomatic way on the computer screen to demarcate the area covered by the growing neurites. The radius of such a circumferential line was then taken as a measure of the extent of neurite growth.

Neurite length was measured either immediately after injection of the HCRP2 antisense mRNA (using 300 mM KCl as a control) and at the 24 and 48 hr time points; values were normalized to the mean length measured at the 24 hr time point in control preparations. In addition, measures were made 12, 36, and 60 hr after cell plating on different substrates; in this case, the obtained values were normalized to the mean length measured in the poly-L-lysine substrate cultures at the 12-hr time point. The data are expressed as mean values ± SEM. Statistical analysis was performed by using two-way repeated-measures ANOVA, followed by multicomparison Newman Keuls test.

RESULTS

Cloning of HCRP1 and HCRP2

To address the topic of the overall structural organization of the HCRPs (Milanese et al.,2008), in this study we report on the isolation of their full-length cDNAs. The 960-bp HCRP cDNA (clone 9.1), previously selected from a *Helix pomatia* nervous tissue expression library using the mouse F3/contactin antibody probe (Milanese et al.,2008) was extended by 5′- and 3′RACE/PCR to 3.5 kb to get a full-length cDNA, which we called "HCRP1," the sequence of which is reported in Figure 1A.

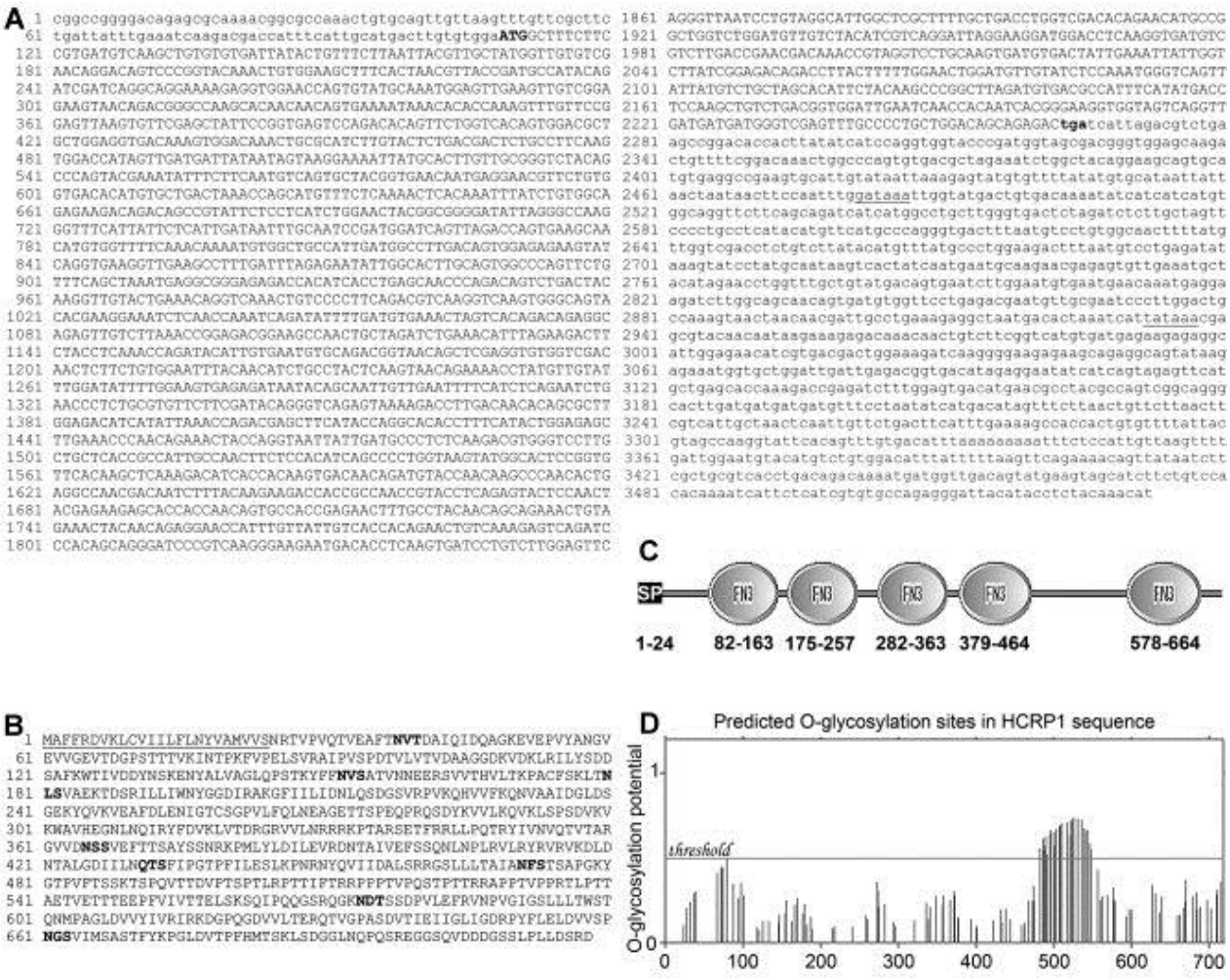

Figure 1. Sequence of the HCRP1 cDNA and structure of the HCRP1 protein. A: Nucleotide sequence of HCRP1 cDNA. The isolated sequence corresponds to a full-length cDNA and includes 5′ (nt 1–108) and 3′ (nt 2,264–3,532) untranslated regions as well as a 2,154–bp open reading frame. The sequence also includes two polyadenylation consensus motifs, 2,481–2,486 and 2,932–2,937 (underscored). B,C: Conceptual translation and domain organization of HCRP1. The HCRP1 protein includes a 718-amino acid protein (B) with a signal peptide (aa 1–24; underscored in B), eight consensuses for N-linked glycosylation (boldface in B), and five fibronectin type III domains (C). D: O-glycosylation sites prediction in the HCRP1 sequence. A stretch of consensus for O-glycosylation was observed in the region between FNIII domains 4 and 5.

The 3,532-nucleotide sequence included a 2,157-bp open reading frame starting at position 109, with two polyadenylation consensus motifs in positions 2,481–2,486 and 2,932–2,937 (Fig. 1A, underscored).

Conceptual translation of this cDNA (Fig. 1B) revealed a 718-amino acid protein, whose domain organization was analyzed with the SMART program (Schultz et al., 1998). A typical N-terminal signal peptide (Bendtsen et al.,2004) spanning amino acids 1–24 (Fig. 1B, underscored) was identified, although no transmembrane region or sequence for membrane attachment via GPI anchor could be detected. In addition, HCRP1 included five fibronectin type III repeats (Fig. 1C; positions 82–163, 175–257, 282–363, 379–464, and 578–664) and carried eight sites for potential N-glycosylation (boldface in Fig. 1B; N positions 38, 152, 180, 365, 430, 471, 574, and 661). A stretch of potential O-glycosylation sites could be predicted between FNIII domains 4 and 5 using the NetOGlyc program of the ExPASy proteomic tool (Fig. 1D), suggesting that N-linked (Milanese et al.,2008) as well as O-linked sugars contributed to the HCRP1 size.

Because previous biochemical analysis identified different HCRPs isoforms in *Helix* nervous tissue extracts (Milanese et al., 2008), we wanted to check whether these proteins could represent the translation products of different mRNAs. Toward this aim, the *Helix* ganglia cDNA expression library was further screened by hybridization with a 980-bp HindIII/XhoI probe, corresponding to the 5′ end of the HCRP1 cDNA. This led to the isolation of clone 8.4.2, bearing a 1.8-kb insert, whose sequence revealed a 1215-bp ORF (Fig. 2A), starting at nt 109, with a polyadenylation consensus at nt 1,471–1,476 (underscored in Fig. 2A). This clone was called "HCRP2." Conceptual translation of the isolated sequence revealed a 405-amino acid protein (Fig. 2B) whose domain organization, studied by the SMART program, included a signal peptide (amino acids 1–24, underscored in Fig. 2B) followed by three FNIII domains (positions 82–163, 172–254, and 262–345; Fig. 2C). Within the protein sequence, four sites for N-linked glycosylation were found in positions 38, 152, 243, and 362 (boldface in Fig. 2B), whereas no consensus for O-glycosylation could be detected.

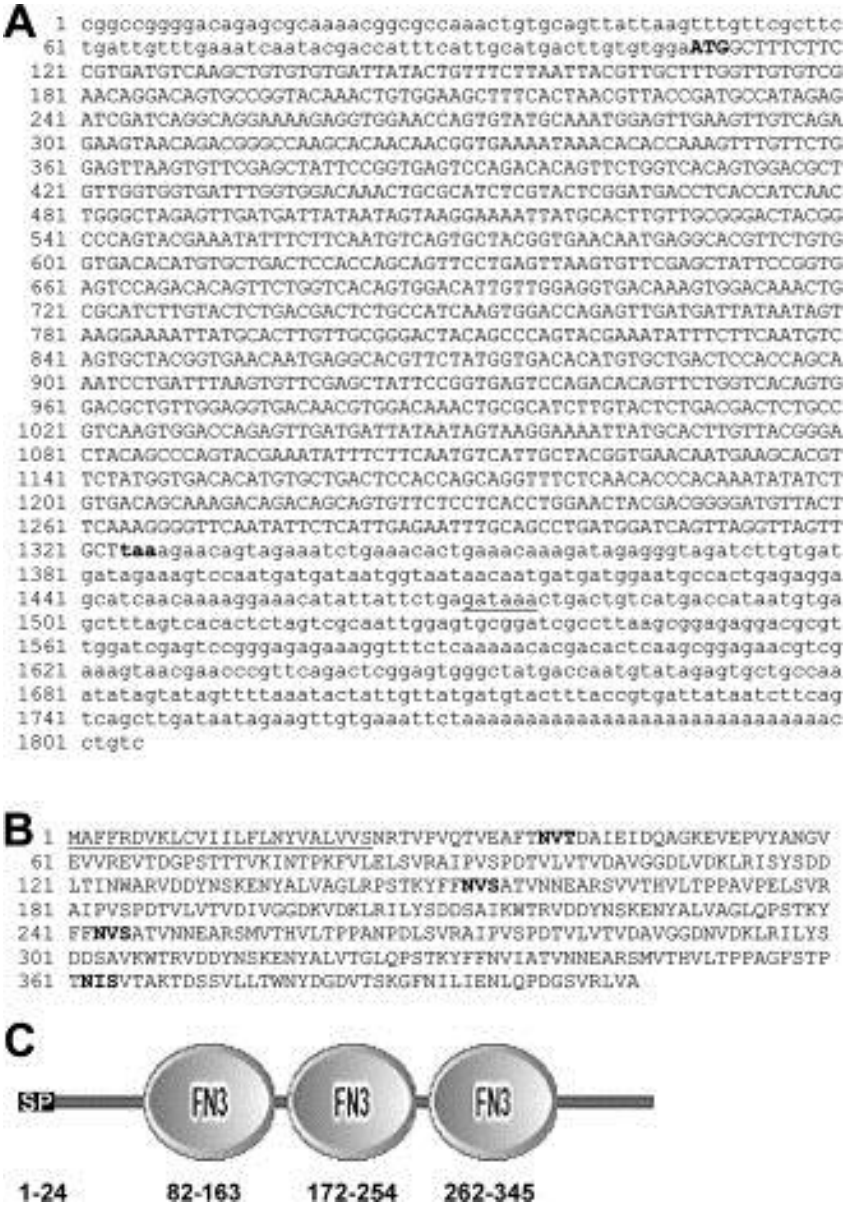

Figure 2. Sequence of the HCRP2 cDNA and structure of the HCRP2 protein. **A:** The full-length sequence of the HCRP2 cDNA includes 5′ (nt 1–108) and 3′ (nt 1,324–1,805) untranslated regions and a 1,215-bp open reading frame. A polyadenylation consensus is found at nt 1,471–1,476 (underscored). **B,C:** Conceptual translation revealed a 405-amino acid sequence (B) including a signal peptide (aa 1–24; underscored in B), four N-glycosylation sites (boldface), and three fibronectin type III repeats (B,C).

Therefore, based on the sequence data, HCRPs included two glycosylated proteins built of FNIII domains, but differing in molecular size. Their calculated molecular masses were 78,931.67 and 45,829.93, respectively. As previously indicated, in *Helix* nervous tissue, F3/contactin antibodies recognize molecular species of 90, 200, and 240 kD, and deglycosylation studies (Milanese et al.,2008) indicated the former as the main HCRP protein backbone, with the higher Mr chains likely arising by posttranslational processing. The deglycosylated HCRP of 90 kD was therefore close to the one predicted from the HCRP1 cDNA. On the other hand, HCRP2 corresponded to a previously undetected protein isoform (see below).

Sequence Comparison

To compare the domain organization of HCRP1 and HCRP2, their amino acid sequences were aligned by using the LALIGN program (Fig. 3). High scores were found by comparing the N-terminal region of HCRP1 with the whole HCRP2 sequence (score 1035; 55.4% identity). The similarity essentially concerned the region including the signal peptide and the first FNIII domain (amino acids 1–170; Fig. 3A), but high scores were also obtained when the first HCRP1 was aligned with the second and third HCRP2 domains (scores 723 and 577; 68.4% and 56.3% identity, respectively; Fig. 3B,C). On the other hand, a sharp drop was found when the following HCRP1 domains were aligned with HCRP2, as confirmed by the graphic output of the results (Fig. 3D). Therefore, the sequence of the first HCRP1 domain was highly conserved among HCRPs, whereas the downstream-located ones displayed lower conservation.

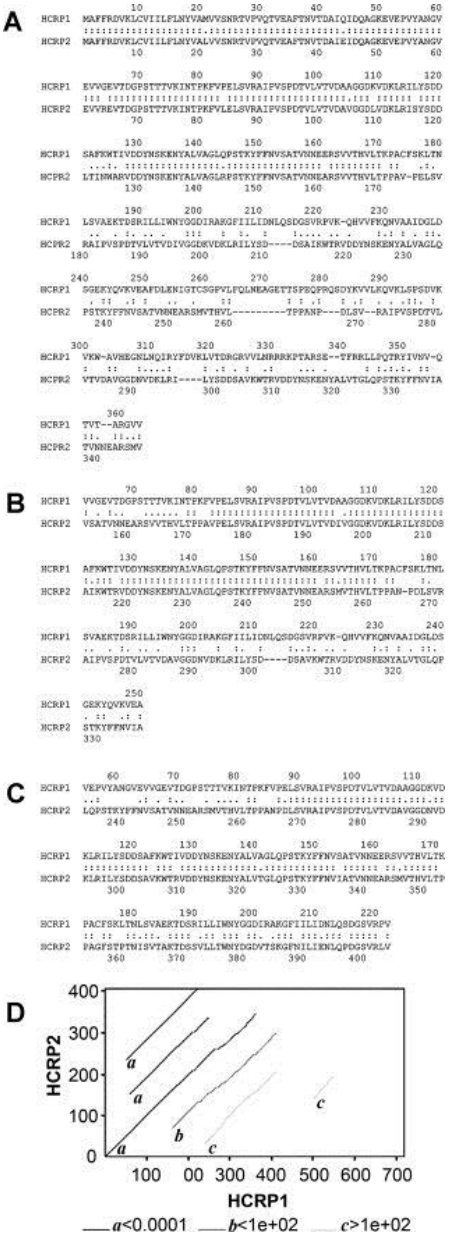

Figure 3. Alignment of the HCRPs sequences. Amino acid sequences were aligned by using the LALIGN program. High similarity was observed between the N-terminal regions of HCRP1 and HCRP2 (**A**), which included the signal peptide

and the first FNIII domain. Similar scores were obtained when the first HCRP1 FNIII domain was aligned to the second (**B**) and third (**C**) HCRP2 domains. The level of similarity dropped sharply when the next HCRP1 domains were compared with the HCRP2 sequence, as deduced from the graphic output of the alignments (**D**).

Distribution of HCRPs in *Helix* Nervous Tissue

To explore further the biological properties of the identified molecules, an anti-HCRPs serum (PF3 serum) was raised in rabbits against a 15-amino acid sequence shared by both HCRPs in their first FNIII domain (positions 111–125). On sections from *Helix* cerebral ganglia, the staining profile of the PF3 serum was indistinguishable from that previously observed with the anti-mouse F3/contactin antibodies (Milanese et al.,2008), demonstrating labelling of neuropil (Fig. 4A1, arrows), cell bodies, and processes (Fig. 4A2). The specificity of the immunostaining profile was deduced from several lines of evidence: 1) no labelling was found on nonnervous tissue, 2) the immunostaining varied from cell to cell (Fig. 4A2, arrowheads) and within the same cell was concentrated on the proximal axonal segment (Fig. 4A2, arrows), and 3) no labelling was observed within the nuclei.

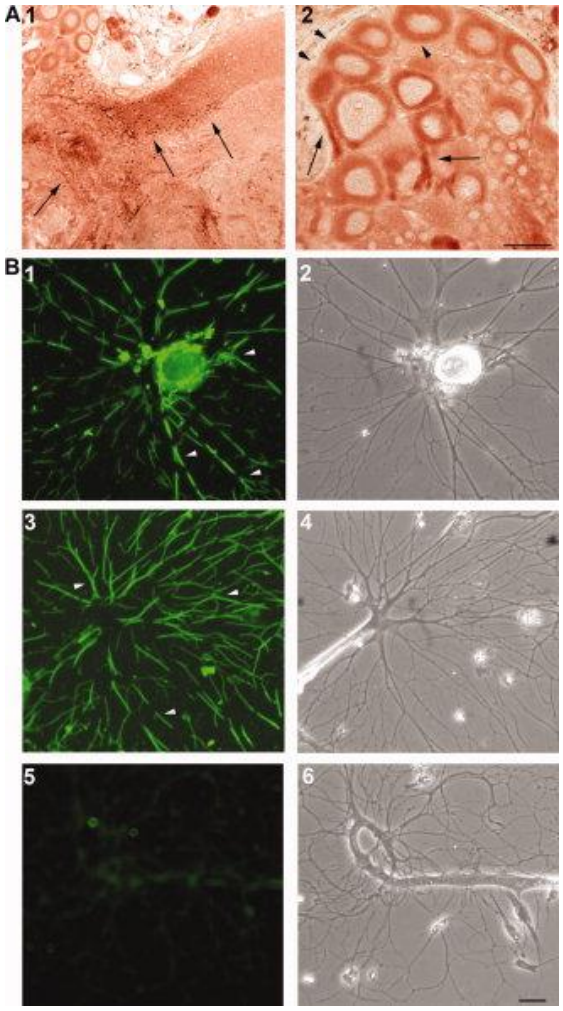

Figure 4. Immunostaining with the anti-HCRPs serum on *Helix pomatia* nervous system. **A:** On sections from *Helix* cerebral ganglia, a variable expression was found in the neuropil (arrows in 1), on cell bodies (arrowheads in 2), and on axons, in which the immunostaining was predominant in the proximal region (arrows in 2). **B:** Strong immunoreactivity on cell bodies (1) and processes (1,3) of cultured neurons. The expression profile appeared occurring at irregular intervals,

with stained region localized along the neurites and at the axonal branching points (arrowheads in 1,3). No staining was observed when the antibody was preincubated with the immunogenic peptide before use (5). Phase-contrast images 2,4,6 represent the same fields as 1,3,5. Scale bars = 100 μm in A1; 50 μm in A2,B.

On cultures from the cerebral ganglia, the PF3 serum stained neuronal cell bodies and processes (Fig. 4B1,3). HCRPs distribution within the neurites was not uniform but restricted to specific axonal segments flanked by immunonegative regions. This profile was similar to the one observed by Milanese et al. (2008) with the same type of cultures with the mouse F3/contactin antibodies. In addition, most of the stained regions appeared close to the neurites branching points (Fig. 4B1,3, arrowheads), suggesting a modulation of the HCRPs cell surface expression that will be the object of further analysis.

To confirm the immunostaining specificity, the PF3 serum was preadsorbed with the immunogenic peptide, which resulted in a complete absence of signal in the stained cells (Fig. 4B5). In addition, no staining was observed when the preimmune serum was used (not shown).

HCRP Molecular Forms

The anti-HCRPs serum specificity was also studied by Western blot. In detergent extracts from *Helix* ganglia, components of 200 and 90 kD were detected, the latter appearing as a doublet of closely spaced bands (Fig. 5A, RIPA). The same profile has been previously observed in *Helix* nervous tissue using the mouse F3/contactin antibodies (Milanese et al., 2008).

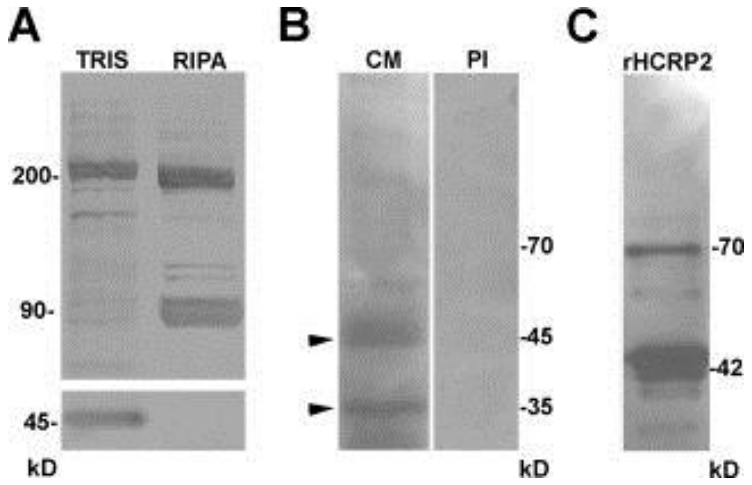

Figure 5. Identification of HCRPs on *Helix* nervous system extracts by Western blotting. **A:** A 200-kD component was identified in both isotonic (Tris) and detergent (RIPA) *Helix* ganglia extracts. A 90-kD band was found in the membrane (RIPA) fraction as a doublet, whereas the 45-kD chain was detected only in the isotonic fraction. **B:** A 45-kD component was detected by the PF3 serum in the *Helix* ganglia-conditioned medium (CM), together with a lower molecular weight band at 35 kD (arrowheads, left lane). No signal was detected when the preimmune serum (PI) was used (right lane). **C:** The profile of the purified GST-HCRP2 fusion protein after GST-tag cleavage is shown. PF3 serum was used. A minor 70-kD component was detected with the 42-kD band, corresponding to the uncleaved fusion protein.

In the isotonic fraction, a 200-kD band with a slightly lower electrophoretic mobility was observed (Fig. 5A, Tris), suggesting that this chain could undergo secretion or shedding from the cell surface.

On the other hand, no 90-kD chain could be found in this fraction, suggesting that the latter corresponded to an intracellular or membrane-associated protein not exported to the cell surface.

A 45-kD component was observed in the isotonic, but not in the membrane-associated, fraction (Fig. 5A, Tris), indicating that this protein could be released in a soluble form. To verify this, we searched the HCRPs presence in the ganglia-conditioned medium (CM), obtained by incubation of *Helix* nervous tissue in culture medium for several days (Fiumara et al., 2005). After 72 hr of incubation, the medium was concentrated and probed by Western blotting with the PF3 antiserum. Under these conditions, a 45-kD band was identified together with a smaller component at 35 kD (Fig. 5B, arrowheads), and no signal was obtained with the preimmune serum (Fig. 5B, PI). Based on its size, the 45-kD isoform could correspond to the translation product of the HCRP2 mRNA, whereas the 35-kD element could represent either an incomplete glycosylation variant of the 45-kD component or a degradation product of the higher Mr chain isoforms during the incubation.

Generation of Recombinant HCRP2

To verify whether the 45-kD chain represented the translation product of the HCRP2 mRNA, GST-HCRP2 fusion proteins were generated, expressed in *E. coli*, and column purified. After cleavage of the GST sequence, E. coli-expressed proteins were analyzed by Western blotting with PF3 antiserum.

As shown in Figure 5C, PF3 antibodies identified a band of 42-kD, close to the HCRP2 predicted size. On the other hand, no band was observed when the preimmune serum was used (not shown). Minor bands of lower molecular size were identified, probably derived from partial degradation of the recombinant proteins, together with a 70-kD component likely corresponding to the residual uncleaved GST-HCRP2 fusion protein. These data further supported the hypothesis that the 45-kD element represented the translation product of the HCRP2 cDNA.

Expression of the HCRP cDNAs in Cell Lines

The above-mentioned data indicated the existence of two main HCRP isoforms, detected by cDNA cloning. The chains of 90- and 45-kD corresponded in size to the translation products of the two isolated HCRP1 and HCRP2 cDNAs, which could represent full-length sequences. To verify this possibility, we used the bicistronic pIRES-EGFP expression vector (Clontech), which included an EGFP reporter downstream of an internal ribosomal entry sequence (IRES). Two different constructs were generated including the HCRP cDNA (either 1 or 2) upstream the IRES-EGFP sequence, both under the control of the same CMV promoter.

After transfection in the LR-73 CHO cell line (Pollard and Stanners, 1979), strong HCRP1 (Fig. 6A) and HCRP2 (Fig. 6D) expressions were detected on fixed cells with PF3 antiserum, and concomitant EGFP expression was revealed through its intrinsic green fluorescence (Fig. 6B,E). PF3 staining indicated that both HCRP1 and HCRP2 were expressed at the cell surface (arrows in Fig. 6A,D), thus reproducing the profile observed in fixed *Helix* neurons (Fig. 4B). On the other hand, the reporter EGFP showed the expected cytoplasmatic localization. Because these proteins were controlled by the same promoter, their expression profiles could be compared (as shown in merged pictures in Fig. 6C,F).

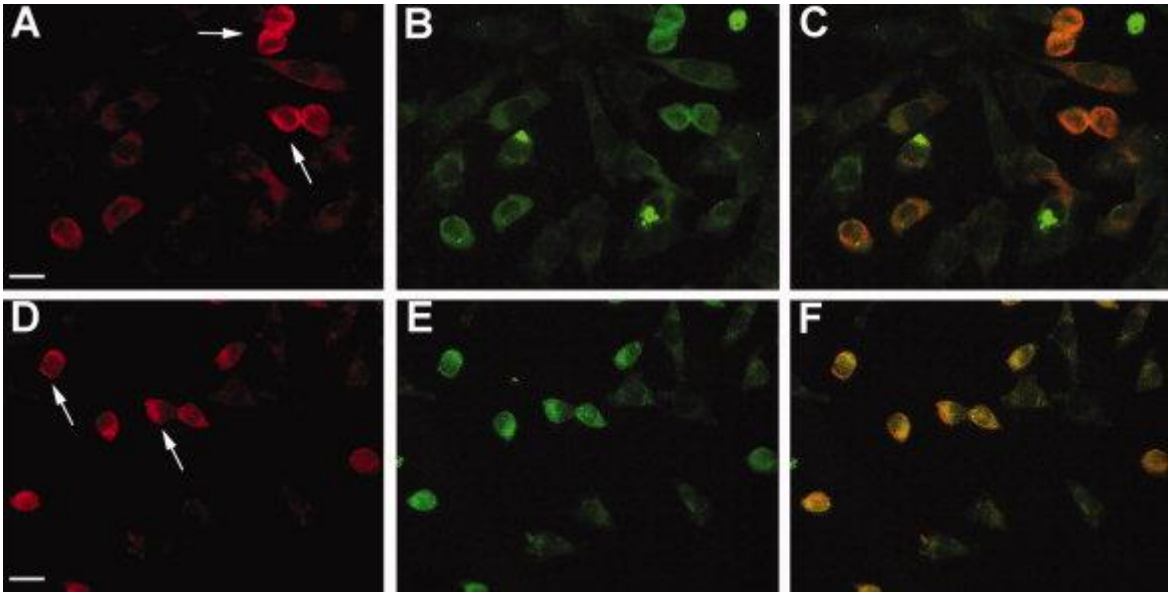

Figure 6. Expression of HCRP cDNAs on transfection in CHO cells. Expression of HCRP1 (**A**), HCRP2 (**D**), and EGFP (**B,E**) upon transfection of pIRES-EGFP expression vector in the LR73 CHO cell line. PF3 serum staining indicated a cell-surface distribution of both HCRPs (arrows in A,D). EGFP expression was identified by its intrinsic fluorescence (B,E). **C** and **F** are merged pictures of A,B and D,E, respectively. Scale bars = 50 μm.

HCRP2 Antisense Inhibits Neurite Growth In Vitro

We previously demonstrated that neurite extension from *Helix pomatia* neurons was strongly inhibited by mouse F3/contactin antibodies (Milanese et al.,2008), which led us to assume that HCRPs were involved in this process. Because the PF3 serum did not recognize the HCRPs native form, we planned to counteract the expression of these proteins in cultured neurons by injecting an antisense mRNA generated from the HCRP2 sequence. In these experiments, EGFP antisense mRNA, previously demonstrated to be devoid of any effect on neurite growth (data not shown), was used as a negative control.

C1 and C3 neurons isolated from *Helix* cerebral ganglia were plated with their initial axonal segment and left to adhere to the substrate for 6–12 hr. At this time, the cells were microinjected with 0.5 μg of antisense mRNA and then allow to grow ON. Neurite length was then measured in both antisense mRNA-treated (n = 14) and control (n = 13; injected with 300 mM KCl) cells. As can be deduced from Figure 7A, the antisense-injected cells displayed reduced neurite length, with significantly lower values already at the 24 hr time point (mean value 62.82% ± 8.18% compared with the control group; $P < 0.05$). At 48 hr, neurite elongation in antisense-treated cells was strongly reduced (95.5% ± 20.8%) compared with the control group (178.47% ± 19.12%; $P < 0.001$). To account for the effects of the HCRPs already expressed by cultured neurons at the time of antisense RNA injection, protein synthesis was temporary inhibited for 10 hr before antisense injection by the bath application of 10 μM anisomycin, starting 6 hr after plating. Although anisomycin treatment reduced per se the extent of axonal elongation (mean values 36.46% ± 5.08% at 24 hr, and 68.18% ± 9.29% at 48 hr compared with control; n = 28; $P < 0.001$), axonal growth in cultures treated at the same time with antisense RNA was almost completely prevented (mean values 17.27% ± 5.08% at 24 hr and 36.4% ± 7.1% at 48 hr compared with control; n = 25; $P < 0.001$). Together these data clearly indicated that HCRPs antisense exerted a sharp inhibiting effect on neurite elongation.

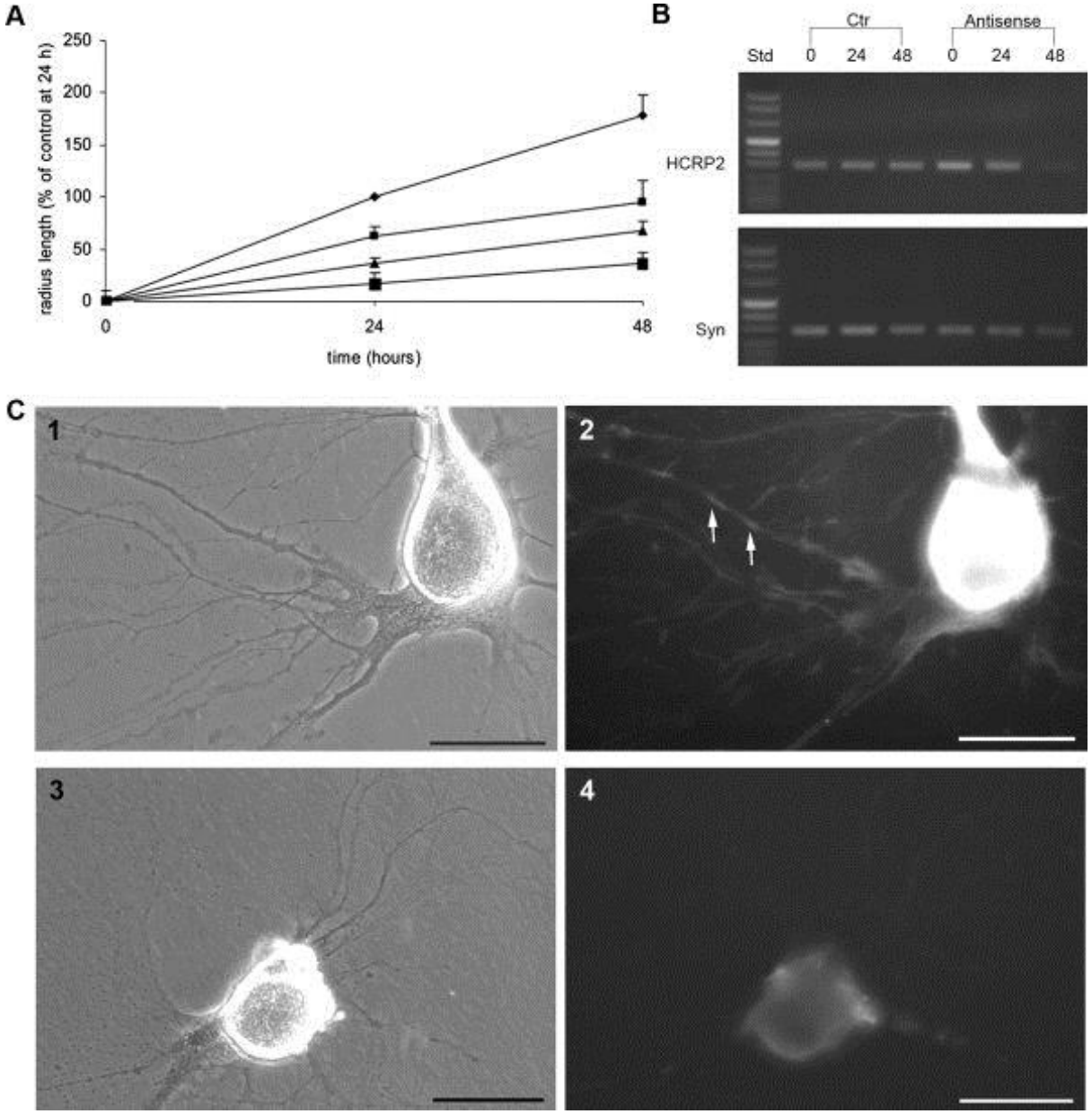

Figure 7. HCRP2 mRNA antisense injection affects neuronal growth in *Helix* cultured neurons. **A:** Graphic representation of neurite elongation in neurons microinjected with antisense HCRP2 mRNA (small squares) or with 300 mM KCl as a control (lozenges). Under both conditions, neurite length was measured also in the presence of anisomycin to account for the contribution of ongoing protein synthesis (triangles, control and anisomycin; large squares, antisense and anisomycin). The cultures were observed 24 and 48 hr after injection. Quantitative data were expressed as percentage mean value (±SEM) of radius length normalized to the control mean value measured at the 24 hr time point. Two-way repeated-measures ANOVA indicated a significant effect between treatments [$F(1,25) = 28.86$, $P < 0.001$] and time [$F(2,50) = 56.999$, $P < 0.001$] and a significant interaction between time and treatments [$F(2,50) = 5.064$, $P = 0.003$]. **B:** Individual B2 microinjected neurons were analyzed for the HCRP2 expression level at the 0, 24, and 48 hr time points by the single-cell RT-PCR. A progressive reduction in HCRP2 transcript is observed in the antisense-injected cells (antisense) compared with the control (Ctr) group, whereas no differences were found in the expression of the synapsin gene in either the control or the antisense-treated cells. **C:** HCRP2 immunoreactivity observed in C3 neurons of *H. pomatia* in the control condition (C2) and 48 hr after antisense injection (C4). Although the typical HCRP2 patchy distribution (arrows) is observed in the control cell, no signal is detected in the antisense-injected neuron. Phase-contrast images of the same fields are shown in C1 and C3, respectively. Scale bars = 50 μm.

Antisense Injection Decreases the HCRP2 Expression

To verify the specificity of the injected antisense in reducing the expression levels of HCRP2, we performed single-cell RT-PCR on both control and antisense-treated C1, B2, and C3 *H. pomatia* neurons at the 0, 24, and 48 hr time points. As indicated in Figure 7B, we found a progressive reduction of the HCRP2 transcript in the antisense-injected cells during the observation. Although in the control group (Ctr) a comparable HCRP2 expression at all the three time points was obtained, in the antisense-treated cells the HCRP2 level showed a slight decrease between time points 0 and 24 hr, and almost disappeared 48 hr after the injection. As an internal control of the reaction, the cells were examined for *Helix* synapsin (AY533823) expression. At each time point, similar levels in both control and treated groups were found (Fig. 7B), confirming that the antisense injection affected the HCRP2 expression in specific manner.

In addition, we wanted to check the HCRP2 protein expression level at the neuronal cell surface after the antisense application. Toward this aim, control and antisense-treated neurons were fixed after 48 hr from the injection and stained with the anti-HCRP2 serum. As shown in Figure 7C4, we demonstrated that the labelling had totally disappeared from the surface of the antisense-treated neurons, whereas control cells showed the typical HCRPs patchy distribution described in previous results (Fig. 4; Milanese et al., 2008). Because the HCRP2 antibody was raised against a peptide sequence partially shared by the HCRP1, the complete disappearance of the immunostaining on antisense-injected neurons allows us to suggest that the HCRP2 mRNA interference also affected the HCRP1 transcript expression. The high homology level described between the two HCRP isoforms (Fig. 3) supports this hypothesis, and further investigations will be performed.

Substrate-Bound HCRP2 Promotes Neurite Extension

Our previous data (Milanese et al., 2008) and the above-described results allowed us to correlate HCRPs expression with neurite elongation. In addition, the presence of HCRP2 in the ganglia-conditioned medium and in the isotonic extracts from *Helix* nervous system supported the hypothesis that HCRP2 could exert its biological effects in a substrate-bound form. To verify this, plastic dishes were coated with purified recombinant HCRP2 or poly-L-lysine, respectively, and the recombinant protein binding to the plastic substrate was monitored by enzyme-linked immunosorbant standard assay (ELISA) using the PF3 antiserum (not shown). Then, C1 and C3 neurons were plated with their initial axonal segment and left to adhere to the substrate for 6–12 hr, and then the growth rate was monitored over 60 hr.

Visual observation of growing neurites at 12, 36, or 60 hr in vitro revealed a sharp increase in their length on the HCRP2 substrate compared with poly-L-lysine (Fig. 8A–D). Quantitative data (Fig. 8E) confirmed this evidence, insofar as the mean growth value registered in cultures plated on HCRP2 substrate at 12 hr was 228.518% ± 19.066% ($n = 39$) of the value measured from cells grown on the poly-L-lysine substrate, taken as the control group ($n = 16$; $P < 0.001$). The differences became then stronger at the following time points. At 36 hr neurite length on the HCRP2 substrate reached a mean value of 327.477% ± 30.266% ($n = 39$; Fig. 8C), whereas, on poly-L-lysine, the value was 140.119% ± 11.388% (Fig. 8A; $n = 16$; $P < 0.001$). The differences still increased at the 60 hr time point (Fig. 8B,D), when the mean value measured on neurons cultured on HCRP2 was 439.542% ± 45.481% ($n = 39$), compared with cells grown on poly-L-lysine, for which a mean length of 148.765% ± 20.436% ($n = 16$; $P < 0.001$) was noted. Similar results were obtained when HCRP2-induced neurite extension was compared with growth on untreated plastic substrate (data not shown), indicating a strong ability of HCRP2 in promoting neurite elongation.

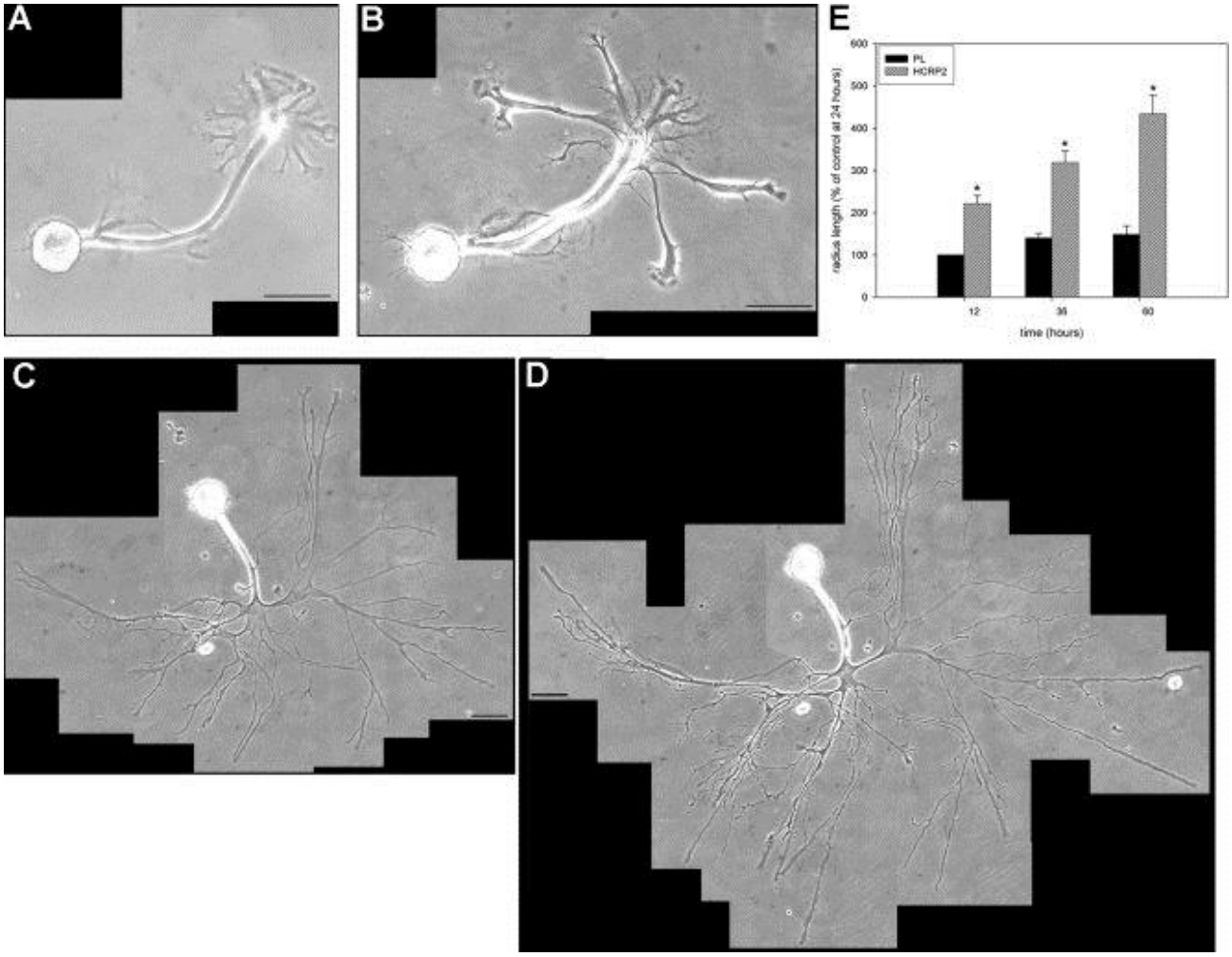

Figure 8. Neurite elongation in *Helix* neurons cultured on different substrates. **A–D:** Phase-contrast images of C3 neurons cultured on poly-L-lysine (A,B) or on HCRP2 (C,D) substrates at the 36 (A,C) and 60 (B,D) hr time points. Longer neurites developed on the HCRP2 substrate, and they displayed a higher level of branching**. E:** Graphic representation of neurite elongation from neurons cultured on HCRP2 or poly-L-lysine (PL) substrates at different time points. Quantitative data were expressed as percentage mean value (± SEM) of radius length normalized to the mean value measured on PL at the 12-hr time point, used as control. Two-way repeated-measures ANOVA showed a significant effect between treatments [$F(1,53) = 16.018$, $P < 0.001$] and time [$F(2,106) = 18.001$, $P < 0.001$] and a significant interaction between time and treatments [$F(2,106) = 6.633$, $P = 0.002$]. Scale bars = 50 μm.

In addition, we tested the effects of substrate-bound HCRP2 on *Helix* neurons cocultured in a soma–soma configuration (Haydon, 1988; Feng et al.,1997,2000; Fiumara et al., 2005), where neuronal cells were paired after the retraction of their neuritic arborization. In this culture condition, neurons plated on poly-L-lysine substrate assumed a particular morphological aspect in which spherical somata were strongly interconnected and neurites projected from one cell to the other, with minimal interactions with the substrate. Interestingly, when soma–soma pairs were plated on an HCRP2-coated dish (n = 15), we observed a flattening of the cell bodies to the bottom of the dish, with a massive arborization growth starting a few hours after plating, favoring cell–substrate adhesion and leading to a progressive separation of the two soma (Fig. 9C,D). Otherwise, soma–soma paired neurons cultured on poly-L-lysine presented their typical spherical morphology and failed to exhibit neurite outgrowth (n = 10; Fig. 9A,B).

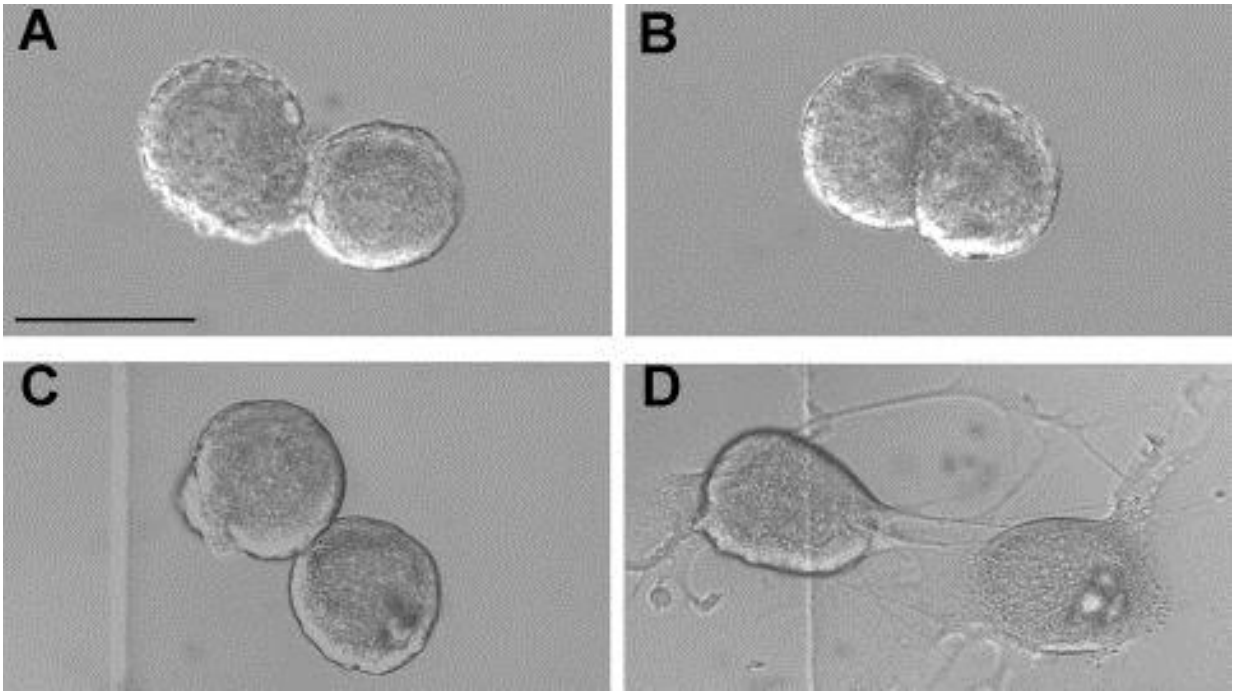

Figure 9. Substrate-bound HCRP2 counteracts the neurite growth inhibition showed by *Helix* neurons in the soma–soma culture configuration. **A,B:** Paired B2–B2 neurons plated on poly-L-lysine substrate immediately after plating (A) and after 24 hr (B). Adhesion between cells increased with time, and no neurite sprouting was visible after 24 hr**. C,D:** Paired B2–B2 neurons plated on HCRP2-coated dish immediately after plating (C) and 24 hr later (D). Interactions between cells progressively decreased, and neurite sprouting occurred after a few hours. Twenty-four hours later, the soma were considerably outdistanced, and growing neurites developed an extended arborization (D). Scale bar = 100 μm.

Previous studies demonstrated that trophic factors released by *Helix* nervous systems incubated in culture medium can modulate synaptogenesis between *Helix* neurons promoting the formation of chemical excitatory synapses and reducing the occurrence of electrical coupling on paired neurons (Fiumara et al.,2005). Because we found the presence of HCPR2 in the conditioned medium, we performed preliminary electrophysiological recordings from the *Helix* B2–B2 neurons pairs in the soma–soma configuration plated on HCRP2 substrate to analyze its hypothetical involvement in the synaptogenesis process. With 46 recorded B2–B2 neurons pairs, we did not observe any change induced by HCRP2 on the chemical/electrical synapses rate compared with the results obtained with neurons cocultured on poly-L-lysine substrate (data not shown).

DISCUSSION

We report on the structural properties and on a further functional characterization of the HCRPs, previously identified in the nervous tissue of the land snail *H. pomatia*, which mediate cell adhesion to the substrate and modulate neurite growth (Milanese et al.,2008). For both attempts, full-length HCRP cDNAs were isolated.

HCRPs Structural Properties

cDNA cloning revealed that HCRPs include two glycoproteins, built of three to five fibronectin type III domains and carrying both N-linked sugars and consensus motives for O-glycosylation. Furthermore, these molecules bear sequence similarities to vertebrate FNIII domain-carrying molecules, including receptor protein tyrosine phosphatases (Tagawa et al., 1997; Oganesian et al., 2003), Nr-CAM (Kayyem et al., 1992), and tenascin N (Tucker et al.,2006). The absence of membrane anchoring sequences and the presence of a typical signal peptide (Bendtsen et al., 2004) support the view that HCRPs represent secreted glycoproteins, in agreement with the evidence that soluble components are detected in *Helix* ganglia isotonic extracts and in the medium conditioned with *Helix* nervous system. The expression of HCRPs at the neuronal surface could be ascribed to their cis interaction with cell surface components, indicating that these molecules may also behave as membrane-associated proteins. A similar association has been demonstrated in vertebrates for the closely related axonal glycoproteins F3/contactin (Rios et al.,2003) and TAG-1 (Traka et al.,2003) with the transmembrane components of neurexin families, which may allow the retention of the soluble forms of these molecules to the cell membrane. However, HCRPs may also interact in trans with cell surface receptors via their polysaccharide chain, as reported for many proteoglycans (Hook et al.,1987; Carey,1997; Seidenbecher et al.,2002), with which HCRPs have many features in common, including the high sugar content and the expression profile at the tissue level (Milanese et al.,2008).

Cloning of HCRPs allowed us to produce the anti-HCRPs serum, which identified molecular forms bearing the same size as detected in the previous study (Milanese et al.,2008) by mouse F3/contactin antibodies, with some differences. Indeed, HCRPs were originally described as complex glycosylated proteins including 240-, 200-, and 90-kD chains. The results of N-deglycosylation experiments revealed that N-linked sugars contribute to the size of the 240- and 200-kD components, whereas the 90-kD protein represented the protein backbone (Milanese et al.,2008). In the present study, no 240-kD chain could be detected by the anti-HCRPs serum, the most likely explanation being that this highly glycosylated chain was not recognized by this antibody. The location of the peptide sequence chosen for PF3 serum generation between the first two putative N-glycosylation sites supports the hypothesis that changes in the extent of glycosylation may affect the ability of the PF3 antibodies to bind HCRPs chains. Therefore, the results obtained using first and second generation antibodies are both consistent with the hypothesis that HCRPs heterogeneity results at least in part from differential addition of N-linked sugars. However, the identification of a cluster of O-glycosylation consensus within the HCRP1 sequence, located between FNIII domains 4 and 5, strongly suggests that also O-linked sugars contribute to the HCRP1 molecular size. Based on these observations, the most likely model we can propose for the HCRPs overall structure is represented by a complex of glycoproteins, built by distinct isoforms implying differential addition of O- and N-linked sugars.

In addition to posttranslational modifications, transcriptional or posttranscriptional mechanisms could also be responsible for the HCRPs diversity. Indeed, cDNA cloning revealed the existence of two isoforms, HCRP1 and HCRP2, encoded by two different mRNAs. The former corresponds to a nearly

80-kD protein, quite close to the 90-kD HCRP chain identified by Western blotting (Milanese et al., 2008; this study). On the other hand, HCRP2 was a previously undetected 45-kD protein, which could be demonstrated by the anti-HCRPs serum in the isotonic extracts from the *Helix* nervous system as well as in the medium conditioned with ganglia, indicating that this molecule corresponded to an HCRP component undergoing secretion or shedding from the cell surface. HCRP2 bears a lower number of FNIII domains, which are mostly similar to the first HCRP1 domain, suggesting that signals for HCRPs retention to the cell membrane could be located within the most C-terminal HCRP1 domain. Whether these domains correspond to protein sequences or carbohydrate chains will be a matter for further investigation.

HCRP1 and HCRP2 similarity mostly concerns the whole HCRP2 sequence and the first HCRP1 FNIII domain, whereas the downstream HCRP1 region is divergent and displays low similarity to HCRP2. The evidence that the two HCRP isoforms bear the same signal peptide strongly suggests that their generation depends on alternative splicing events within the same gene. In this case, the identification of a single 6.3-kb HCRP mRNA (Milanese et al.,2008) would imply that this chain included different isoforms bearing similar relative mobility, as reported for the gene encoding the myelin-associated glycoprotein (Erb et al.,2003). Alternative splicing may thus be responsible for the generation of HCRP isoforms undergoing different subcellular distribution, as shown for the myelin basic protein (Gould et al.,1999), the spectrin isoforms (Berghs et al.,2000), and the GluR7 kainate receptor subunits (Jaskolski et al.,2005).

In addition, different glycosylation pathways can regulate proteins processing and may remarkably influence their size, targeting, and functions (Varki,1998). Therefore, the glycosylation heterogeneity observed in the HCRPs may be the cause of their differential partition within different compartments. The occurrence of the 200-kD protein in both soluble and membrane fractions indicates that this higher variant bears the potential to be associated with the cell membrane and also to be delivered in soluble form. On the other hand, the 45-kD component was specifically detected in soluble extracts, and its absence in the membrane fractions could be ascribed to the lack of the full domain repertoire responsible for the cis association with the cell surface. In contrast, the 90-kD chain was never detected in soluble form, and, in agreement with its low sugar content (Milanese et al.,2008), this chain may represent an intracellular component undergoing initial glycosylation during its transit through the endoplasmic reticulum to the cell surface.

Given the above considerations, HCRPs may represent a glycoprotein family built of different chains bearing a modular structure with domains undergoing high glycosylation, responsible for cell surface expression, and domains responsible for cis interactions, which potentially mediate their association with the cell membrane components. These domains may be differentially included in the mature proteins and then result in differential HCRPs subcellular distribution. Further studies will be necessary to elucidate the overall organization of the *HCRP* gene and the mechanism by which the different HCRP isoforms are generated.

HCRPs Structure–Function Relationships

HCRPs are built of a variable number of FNIII domains, ranging from three to five. The lack of further, structurally different functional domains indicates that these sequences are responsible for the described functions and in particular for the control of neurite growth, for which several studies have indicated that FNIII domains are involved (Xiao et al.,1996; Rigato et al.,2002; Gonzalez-Brito and Bixby,2006). Several lines of evidence suggest that FNIII domains play relevant roles in the functions of axonally expressed glycoproteins, as demonstrated for L1 (Pocock et al.,2007) and for

anosmin, the protein encoded by KAL-1, whose mutation is responsible for the X-linked Kallmann's syndrome (Hu et al.,2003).

The significance of the two HCRP isoforms in these functions is obscure. However, the three FNIII domains of HCRP2 are highly homologous to each other, in particular to the first HCRP1 FNIII domain, suggesting that interactions of these domains are likely responsible for the functional effects on neurite growth and on cell adhesion. On the other hand, the downstream HCRP1 domains may rather work as spacers, responsible for HCRP1 cis interactions, which might regulate the observed differential HCRP1 distribution across subcellular compartments.

HCRPs Functional Properties

We previously showed that HCRP antibodies affect neuronal adhesion to the substrate, neurite elongation, and neurotransmitter release (Milanese et al.,2008). In this study, the functional role of HCRPs in neurite elongation was confirmed, insofar as the HCRP2 antisense mRNA was found to exert inhibitory effects on axonal growth from cultured *H. pomatia* neurons, and we also provide evidence that the purified recombinant HCRP2 molecule promotes neurite growth when used as a substrate for growing *Helix* neurons.

Therefore, the significance of HCRPs as neurite growth-promoting molecules could be subsequent to their ability to modulate substrate adhesion as demonstrated in the present work and in previous studies (Milanese et al.,2008), which fits with the results of several studies relating adhesion of neurons to the substrate to the extent of neurite elongation in different systems (Gruenbaum and Carew,1999; Forni et al.,2004).

For *Lymnaea stagnalis*, it has been demonstrated that soma–soma contacts prevented neurite formation even in the presence of the appropriate trophic factors (Feng et al.,2000; Munno et al.,2000). Conversely, we found that the presence of HCRP2 as substrate for paired neurons is sufficient to counteract the strong adhesion established between *Helix* somata juxtaposed in culture (Feng et al.,2000; Fiumara et al.,2005), promoting neurite sprouting and growth in an extended arborization.

Electrophysiological recordings show that HCRP2 substrate failed in the induction of chemical excitatory synapse formation in soma–soma cultures, corroborating the hypothesis that molecules mediating neurite outgrowth are not sufficient for the formation of chemical excitatory synapses in invertebrates (Feng et al.,1997; Woodin et al,1999; Hamakawa et al.,1999; Munno et al.,2000; Fiumara et al.,2005). Taken together, these results show that HCRP2 is directly involved in neurite growth regulation and could mediate its functions, probably activating a signalling pathway, such as the tyrosine kinase systems, as described for several extrinsic growth factors (Shelessinger and Ullrich,1992; Hamakawa et al.,1999; Munno et al.,2000; Meems et al.,2003; Fiumara et al.,2005). This hypothesis should imply the presence of HCRPs transmembrane receptors on Helix neurons, whose nature remains to be identified.

Acknowledgements

We thank Dr. Leonarda de Benedictis for her technical help in molecular biology procedures and Dr. Claudio Franchino for his support in cell biology techniques.

REFERENCES

Bendtsen JD, Nielsen H, Von Heijne G, Brunak S. 2004. Improved prediction of signal peptides: SignalP 3.0. *J Mol Biol* **340**:783–795.

Berghs S, Aggujaro D, Dirkx R Jr, Maksimova E, Stabach P, Hermel JM, Zhang JP, Philbrick W, Slepnev V, Ort T, Solimena M. 2000. BetaIV spectrin, a new spectrin localized at axon initial segments and nodes of ranvier in the central and peripheral nervous system. *J Cell Biol* **151**:985–1002.

Berglund EO, Murai KK, Fredette B, Sekerkova G, Marturano B, Weber L, Mugnaini E, Ranscht B. 1999. Ataxia and abnormal cerebellar microorganization in mice with ablated contactin gene expression. *Neuron* **24**:739–750.

Bizzoca A, Virgintino D, Lorusso L, Buttiglione M, Yoshida L, Polizzi A, Tattoli M, Cagiano R, Rossi F, Kozlov S, Furley A, Gennarini G. 2003. Transgenic mice expressing F3/contactin from the TAG1 promoter exhibit developmentally regulated changes in the differentiation of cerebellar neurons. *Development* **130**:29–43.

Boyle ME, Berglund EO, Murai KK, Weber L, Peles E, Ranscht B. 2001. Contactin orchestrates assembly of the septate-like junctions at the paranode in myelinated peripheral nerve. *Neuron* **30**:385–397.

Carey DJ. 1997. Syndecans: multifunctional cell-surface co-receptors. *Biochem J* **327**:1–16.

Colon-Ramos DA, Margeta MA, Shen K. 2007. Glia promote local synaptogenesis through UNC-6 (netrin) signaling in *C. elegans*. *Science* **318**:103–106.

Coluccia A, Tattoli M, Bizzoca A, Arbia S, Lorusso L, De Benedictis L, Buttiglione M, Cuomo V, Furley A, Gennarini G, Cagiano R. 2004. Transgenic mice expressing F3/contactin from the transient axonal glycoprotein promoter undergo developmentally regulated deficits of the cerebellar function. *Neuroscience* **123**:155–166.

Dupree JL, Girault JA, Popko B. 1999. Axo-glial interactions regulate the localization of axonal paranodal proteins. *J Cell Biol* **147**:1145–1152.

Durbec P, Gennarini G, Buttiglione M, Gomez S, Rougon G. 1994. Different domains of the F3 neuronal adhesion molecule are involved in adhesion and neurite outgrowth promotion. *Eur J Neurosci* **6**:461–472.

Erb M, Steck AJ, Nave KA, Schaeren Wiemers N. 2003. Differential expression of L- and S-MAG upon cAMP stimulated differentiation in oligodendroglial cells. *J Neurosi Res* **71**:326–337.

Feng ZP, Klumperman J, Lukowiak K, Syed NI. 1997. In vitro synaptogenesis between the somata of identified *Lymnaea* neurons requires protein synthesis but not extrinsic growth factors or substrate adhesion molecules. *J Neurosci* **20**:7839–7849.

Feng ZP, Hasan SU, Lukowiak K, Syed NI. 2000. Target cell contact suppresses neurite outgrowth from soma–soma paired *Lymnaea* neurons. *J Neurobiol* **42**:357–369.

Fiumara F, Leitinger G, Milanese C, Montarolo PG, Ghirardi M. 2005. In vitro formation and activity-dependent plasticity of synapses between *Helix* neurons involved in the neural control of feeding and withdrawal behaviors. *Neuroscience* **134**:1133–1151.

Fiumara F, Milanese C, Corradi A, Giovedı` S, Leitinger G, Menegon A, Montarolo PG, Benfenati F, Ghirardi M. 2007. Phosphorylation of synapsin domain A is required for post-tetanic potentiation. *J Cell Sci* **120**:3228–3237.

Forni JJ, Romani S, Doherty P, Tear G. 2004. Neuroglian and fasciclinII can promote neurite outgrowth via the FGF receptor Heartless. *Mol Cell Neurosci* **26**:282–291.

Frangioni JV, Neel BG. 1993. Solubilization and purification of enzymatically active glutatione S-transferase (pGEX) fuson proteins. *Anal Biochem* **210**:179–187.

Funada M, Hara H, Sasagawa H, Kitagawa Y, Kadowaki T. 2007. A honey bee Dscam family member, AbsCAM, is a brain-specific cell adhesion molecule with the neurite outgrowth activity which influences neuronal wiring during development. *Eur J Neurosci* **25**:168–180.

Gennarini G, Durbec P, Boned A, Rougon G, Goridis C. 1991. Transfected F3/F11 neuronal cell surface protein mediates intercellular adhesion and promotes neurite outgrowth. *Neuron* **6**:595–606.

Gerrow K, El-Husseini A. 2006. Cell adhesion molecules at the synapse. *Front Biosci* **11**:2400–2419.

Ghirardi M, Casadio A, Santarelli L, Montarolo PG. 1996. *Aplysia* hemolymph promotes neurite outgrowth and synaptogenesis of identified *Helix* neurons in cell culture. *Invert Neurosci* **2**:41–49.

Ghirardi M, Naretto G, Fiumara F, Vitiello F, Montarolo PG. 2001. Target-dependent modulation of neurotransmitter release in cultured *Helix* neurons involves adhesion molecules. *J Neurosci Res* **65**:111–120.

Gollan L, Salomon D, Salzer JL, Peles E. 2003. Caspr regulates the processing of contactin and inhibits its binding to neurofascin. *J Cell Biol* **163**:1213–1218.

Gonzalez-Brito MR, Bixby JL. 2006. Differential activities in adhesion and neurite growth of fibronectin type III repeats in the PTP-delta extracellular domain. *Int J Dev Neurosci* **24**:425–429.

Gould RM, Freund CM, Barbarese E. 1999. Myelin-associated oligodendrocytic basic protein mRNAs reside at different subcellular locations. *J Neurochem* **73**:1913–1924.

Gruenbaum LM, Carew TJ. 1999. Growth factor modulation of substrate-specific morphological patterns in *Aplysia* bag cell neurons. *Learn Mem* **6**:292–306.

Hamakawa T, Woodin MA, Bjorgum MC, Painter SD, Takasaki M, Lukowiak K, Nagle GT, Syed NI. 1999. Excitatory synaptogenesis between identified *Lymnaea* neurons requires extrinsic trophic factors and is mediated by receptor tyrosine kinases. *J Neurosci* **19**:9306–9312.

Haydon PG. 1988. The formation of chemical synapses between cell-cultured neuronal somata. *J Neurosci* **8**:1032–1038.

Hook M, Kjellen L, Woods A. 1987. Analysis of membrane-associated proteoglycans. *Methods Enzymol* **144**:394–401.

Hu Y, Tanriverdi F, MacColl GS, Bouloux PM. 2003. Kallmann's syndrome: molecular pathogenesis. *Int J Biochem Cell Biol* **35**:1157–1162.

Jaskolski F, Normand E, Mulle C, Coussen F. 2005. Differential trafficking of GluR7 kainate receptor subunit splice variants. *J Biol Chem* **280**:22968–22976.

Kayyem JF, Roman JM, De la Rosa EJ, Schwarz U, Dreyer WJ. 1992. Bravo/Nr-CAM is closely related to the cell adhesion molecules L1 and Ng-CAM and has a similar heterodimer structure. *J Cell Biol* **118**:1259–1270.

Kristiansen LV, Velasquez E, Romani S, Baars S, Berezin V, Bock E, Hortsch M, Garcia-Alonso L. 2005. Genetic analysis of an overlapping functional requirement for L1- and NCAM-type proteins during sensory axon guidance in *Drosophila*. *Mol Cell Neurosci* **28**:141–152.

Lardi-Studler B, Fritschy JM. 2007. Matching of pre- and postsynaptic specializations during synaptogenesis. *Neuroscientist* **13**:115–126.

Latefi NS, Colman DR. 2007. The CNS synapse revisited: gaps, adhesive welds, and borders. *Neurochem Res* **32**:303–310.

Li J, Ashley J, Budnik V, Bhat MA. 2007. Crucial role of Drosophila neurexin in proper active zone apposition to postsynaptic densities, synaptic growth, and synaptic transmission. *Neuron* **55**:741–755.

Maness PF, Schachner M. 2007. Neural recognition molecules of the immunoglobulin superfamily: signaling transducers of axon guidance and neuronal migration. *Nat Neurosci* **10**:19–26.

Mann F, Rougon G. 2007. Mechanisms of axon guidance: membrane dynamics and axonal transport in semaphorin signalling. *J Neurochem* **102**:316–323.

Mayford M, Barzilai A, Keller F, Schacher S, Kandel ER. 1992. Modulation of an NCAM-related adhesion molecule with long-term synaptic plasticity in *Aplysia*. *Science* **256**:638–644.

Meems R, Munno D, van Minnen J, Syed NI. 2003. Synapse formation between isolated axons requires presynaptic soma and redistribution of postsynaptic AChRs. *J Neurophysiol* **89**:2611–2619.

Milanese C, Fiumara F, Bizzoca A, Giachello C, Leitinger G, Gennarini G, Montarolo PG, Ghirardi M. 2008. F3/contactin-related proteins in *Helix pomatia* nervous tissue (HCRPs): distribution and function in neurite growth and neurotransmitter release. *J Neurosci Res* **86**:821–831.

Munno DW, Woodin MA, Lukowiak K, Syed NI, Dickinson PS. 2000. Different extrinsic trophic factors regulate neurite outgrowth and synapse formation between identified *Lymnaea* neurons. *J Neurobiol* **44**:20–30.

Oganesian A, Poot M, Daum G, Coats SA, Wright MB, Seifert RA, Bowen-Pope DF. 2003. Protein tyrosine phosphatase RQ is a phosphatidylinositol phosphatase that can regulate cell survival and proliferation. *Proc Natl Acad Sci U S A* **100**:7563–7568.

Pocock R, Be´nard CY, Shapiro L, Hobert O. 2007. Functional dissection of the *C. elegans* cell adhesion molecule SAX-7, a homologue of human L1. *Mol Cell Neurosci* doi:10.1016/j.mcn.2007.08.014.

Pollard JW, Stanners CP. 1979. Characterization of cell lines showing growth control isolated from both the wild type and a leucyl-tRNA synthetase mutant of Chinese hamster ovary cells. *J Cell Physiol* **98**:571–585.

Rigato F, Garwood J, Calco V, Heck N, Faivre-Sarrailh C, Faissner A. 2002. Tenascin-C promotes neurite outgrowth of embryonic hippocampal neurons through the alternatively spliced fibronectin type III BD domains via activation of the cell adhesion molecule F3/contactin. *J Neurosci* **22**:6596–6609.

Rios JC, Rubin M, St. Martin M, Downey RT, Einheber S, Rosenbluth J, Levinson SR, Bhat M, Salzer JL. 2003. Paranodal interactions regulate expression of sodium channel subtypes and provide a diffusion barrier for the node of Ranvier. *J Neurosci* **23**:7001–7011.

Schacher F, Wu S, Sun ZY, Wang D. 2000. Cell-specific changes in expression of mRNAs encoding splice variants of *Aplysia* cell adhesion molecule accompany long-term synaptic plasticity. *J Neurobiol* **45**:152–161.

Schlessinger J, Ullrich A. 1992. Growth factor signaling by receptor tyrosine kinases. *Neuron* **9**:383–391.

Schultz J, Milpetz F, Bork P, Ponting CP. 1998. SMART, a simple modular architecture research tool: identification of signalling domains. *Proc Natl Acad Sci U S A* **95**:5857–5864.

Seidenbecher CI, Smalla KH, Fischer N, Gundelfinger ED, Kreutz MR. 2002. Brevican isoforms associate with neural membranes. *J Neurochem* **83**:738–746.

Shapiro L, Love J, Colman DR. 2007. Adhesion molecules in the nervous system: structural insights into function and diversity. *Annu Rev Neurosci* **30**:451–474.

Tagawa M, Shirasawa T, Yahagi Y, Tomoda T, Kuroyanagi H, Fujimura S, Sakiyama S, Maruyama N. 1997. Identification of a receptor-type protein tyrosine phosphatase expressed in postmitotic maturing neurons: its structure and expression in the central nervous system. *Biochem J* **321**:865–871.

Traka M, Goutebroze L, Denisenko N, Bessa M, Nifli A, Havaki S, Iwakura Y, Fukamauchi F, Watanabe K, Soliven B, Girault JA, Karagogeos D. 2003. Association of TAG-1 with Caspr2 is essential for the molecular organization of juxtaparanodal regions of myelinated fibers. *J Cell Biol* **162**:1161–1172.

Tucker RP, Drabikowski K, Hess JF, Ferralli J, Chiquet-Ehrismann R, Adams JC. 2006. Phylogenetic analysis of the tenascin gene family: evidence of origin early in the chordate lineage. *BMC Evol Biol* **7**:6–60.

Varki A. 1998. Factors controlling the glycosylation potential of the Golgi apparatus. Trends *Cell Biol* **8**:34–40.

Wang X, Kweon J, Larson S, Chen L. 2005. A role for the *C. elegans* L1CAM homologue lad-1/sax-7 in maintaining tissue attachment. *Dev Biol* **284**:273–279.

Woodin MA, Hamakawa T, Takasaki M, Lukowiak K, Syed NI. 1999. Trophic factor-induced plasticity of synaptic connections between identified *Lymnaea* neurons. *Learn Mem* **6**:307–316.

Xiao ZC, Taylor J, Montag D, Rougon G, Schachner M. 1996. Distinct effects of recombinant tenascin-R domains in neuronal cell functions and identification of the domain interacting with the neuronal recognition molecule F3/11. *Eur J Neurosci* **8**:766–782.

Yamada S, Nelson WJ. 2007. Synapses: sites of cell recognition, adhesion, and functional specification. *Annu Rev Biochem* **76**:267–294.